Tunneling conductance of ferromagnet/noncentrosymmetric superconductor junctions

S. Wu and K. V. Samokhin
Department of Physics, Brock University, St. Catharines, Ontario, Canada L2S 3A1
(Received 17 April 2009; revised manuscript received 4 June 2009; published 22 July 2009)

Based on the extended Blonder-Tinkham-Klapwijk formalism, the tunneling conductance characteristics of a planar junction between a ferromagnet and a noncentrosymmetric superconductor are studied. The effects of the Rashba spin-orbit coupling (RSOC), the exchange energy, and the Fermi wave-vector mismatch (FWM) on the conductance are all taken into account. In the absence of the FWM, it is found that far away from the gap edge the conductance is suppressed by the RSOC while around the gap edge it is almost independent of RSOC. The interplay of the RSOC and the exchange energy causes an enhancement of the subgap conductance, which is more pronounced when the RSOC is small. When the FWM is introduced, it is shown that the conductance is monotonically enhanced as the FWM parameter decreases.

DOI: 10.1103/PhysRevB.80.014516 PACS number(s): 74.50.+r, 74.45.+c

I. INTRODUCTION

In recent years, tunneling spectroscopy has played a crucial role in probing electronic states of superconductors (SCs). In normal-metal/superconductor junctions, zero-bias conductance peaks[1–3] observed in high-temperature superconductors are explained as arising from the sign change in the pair potential, which leads to the formation of midgap surface states. Replacing the normal metal by a ferromagnetic metal, the conductance spectrum is considerably changed due to the spin polarization caused by the exchange field. Earlier works[4–8] have demonstrated that the effect of the exchange energy is, in general, to reduce the Andreev reflection (AR) at a ferromagnet/centrosymmetric superconductor (FM/CSC) interface. So far, a variety of physical phenomena, including the effects of temperature,[9] the planar magnetization components,[10] and the Fermi wave-vector mismatch (FWM) (Refs. 11 and 12) on the tunneling conductance and the proximity effect,[13,14] has been investigated. In particular, in Refs. 11 and 12 the effect of the FWM was considered and it was found that in some cases the exchange energy can enhance Andreev reflection. We would also like to mention Ref. 15, where the tunneling conductance was calculated for an FM/CSC junction in which the FM and SC sides are separated by a two-dimensional electron gas with the Rashba spin-orbit coupling (RSOC).

The recent discovery of superconductivity in the heavy fermion compound $CePt_3Si$ (Ref. 16) has renewed interest, both experimental and theoretical, in the properties of superconductors without inversion symmetry. Noncentrosymmetric superconductors (NCSCs) exhibit a variety of distinctive features, which is absent in the centrosymmetric case, such as a strongly anisotropic spin susceptibility with a large residual component,[17–19] magnetoelectric effect,[20,21] and unusual nonuniform ("helical") superconducting phases.[22–24] The tunneling conductance in a normal-metal/noncentrosymmetric superconductor (N/NCSC) junction has been recently studied in Refs. 25–27. In these works, Yokoyama *et al.*[25] found that an intrinsically *s*-wave-like property of a triplet NCSC results in a peak at the energy gap in the tunneling spectrum. Iniotakis *et al.*[26] observed the zero-bias anomalies if a specific form of the mixed singlet-triplet order parameter was realized. Linder and Sudbø[27] found pronounced peaks and bumps in the conductance spectrum corresponding to the sum and difference of the magnitudes of the singlet and triplet gaps. One of the important questions is how the Andreev reflection affects the tunneling conductance in the presence of *both* ferromagnetism and RSOC. So far, there has been no theory for this phenomenon.

The purpose of this paper is to investigate the tunneling spectroscopy of a ferromagnet/noncentrosymmetric superconductor (FM/NCSC) junction. We employ the well-known Blonder-Tinkham-Klapwijk (BTK) formalism[28] but extend and generalize it to include the effects of the exchange energy (some references called it spin polarization) in the ferromagnet, the RSOC due to the lack of inversion symmetry, and the existence of FWM. We find many interesting features in the conductance spectrum, stemming from the interplay of magnetism and the RSOC. Away from the gap edge, the tunneling conductance is enhanced as the RSOC decreases, while it is almost unchanged near the gap edge. This behavior is completely different from that found in the N/NCSC junction.[25] The competition between the effects of the exchange energy and the RSOC on the AR leads to an enhanced subgap conductance, which can even result in a maximum at zero energy under certain conditions. In addition, we also show the importance of properly accounting for the FWM, namely, the conductance spectrum monotonically increases with decreasing the FWM parameter in the whole excitation-energy region, which is essentially different from the behavior found in the FM/CSC junctions.[11,12,29]

The paper is organized as follows. In Sec. II, we define the theoretical model and extend the BTK approach to obtain the amplitudes for various scattering processes that occur in the FM/NCSC junction. In Sec. III, the corresponding numerical results for the tunneling conductance are presented and discussed. Section IV contains a summary of our results.

II. FORMULATION OF THE MODEL

We consider the tunneling conductance of the FM/NCSC junction as shown in Fig. 1. The FM is at $x<0$ and is described by an effective single-particle Hamiltonian. The NCSC is assumed to have purely singlet pairing and is de-

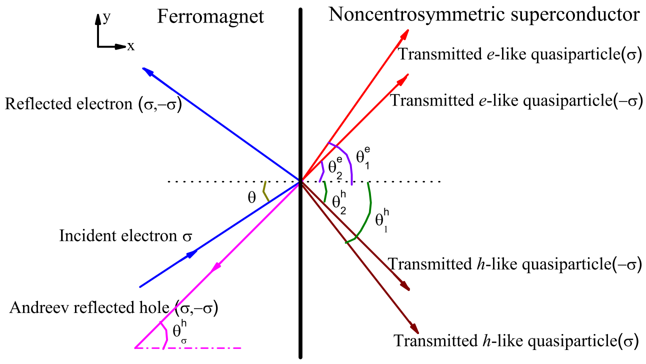

FIG. 1. (Color online) Schematic illustration of the scattering processes at the FM/NCSC interface. The angles of normal and Andreev reflections for electrons and holes with $\sigma=\uparrow,\downarrow$ are different. Due to the presence of spin-orbit coupling, the electronlike and holelike excitations on the superconducting side are scattered through different angles.

scribed by a BCS-like Hamiltonian. The FM/NCSC interface is at $x=0$, where there is interfacial scattering, which is modeled by a potential $U(\boldsymbol{r})=U_0\delta(x)$, with U_0 characterizing the barrier strength. The band dispersions are isotropic and the effective masses of quasiparticles are assumed to be the same on both sides. According to Ref. 30, the effect of the mass difference is equivalent to that caused by a variation in the interface potential strength. The quasiparticle wave function satisfies the following Bogoliubov–de Gennes (BdG) equation:

$$\mathcal{H}\Psi(\boldsymbol{r}) = E\Psi(\boldsymbol{r}), \tag{1}$$

where

$$\mathcal{H} = \begin{pmatrix} \hat{H}(\boldsymbol{r}) - \sigma h(\boldsymbol{r}) & \hat{\Delta}(\boldsymbol{r}) \\ \hat{\Delta}^\dagger(\boldsymbol{r}) & -[\hat{H}^T(\boldsymbol{r}) + \sigma h(\boldsymbol{r})] \end{pmatrix}, \tag{2}$$

with the single-particle Hamiltonian

$$\hat{H}(\boldsymbol{r}) = \left(-\frac{\boldsymbol{\nabla}^2}{2m} + U(\boldsymbol{r}) - E_{Fi} \right)\hat{\sigma}_0 + \gamma(\boldsymbol{k},\boldsymbol{r})\hat{\boldsymbol{\sigma}}.$$

Here $E_{Fi}=E_{\mathrm{FM}},E_{FS}$ represent the Fermi energies in the FM and the NCSC regions, respectively, $\sigma=\pm 1$ for different spin orientations, $h(\boldsymbol{r})=h_0\theta(-x)$ is the exchange energy on the FM side (we assume that the FM magnetization and the exchange energy are along the z axis), $\boldsymbol{\gamma}(\boldsymbol{k},\boldsymbol{r})=\boldsymbol{\gamma}(\boldsymbol{k})\theta(x)$ is the antisymmetric (Rashba) spin-orbit coupling on the SC side, and $\hat{\boldsymbol{\sigma}}$ are the Pauli matrices (we use the units in which $\hbar=1$). We discuss only the clean case with specular scattering at the interface. Taking disorder into account, both in the bulk and at the interface, is beyond the scope of the BTK formalism.

In our model, we consider a noncentrosymmetric superconductor with the tetragonal crystal symmetry, which is relevant for $CePt_3Si$, $CeRhSi_3$, and $CeIrSi_3$. We choose the RSOC in the following form: $\boldsymbol{\gamma}(\boldsymbol{k})=\gamma_0(k_y,-k_x,0)$ with the Rashba coupling constant γ_0 and the BCS pairing potential $\hat{\Delta}(\boldsymbol{r})=i\hat{\sigma}_y\Delta_0\theta(x)$. We take into account the fact that the Fermi energy is different in the FM and NCSC regions, which allows for different bandwidths originating from different carrier densities in the two regions. We introduce the dimensionless FWM parameter as follows: $R=k_{FS}/k_{\mathrm{FM}} \equiv \sqrt{E_{FS}/E_{\mathrm{FM}}}$. In Sec. III we will show that the FWM between the two regions plays an important role in the tunneling conductance.

We focus on the excitations with $E\geq 0$, assuming an incident electron above the Fermi level. When an electron is injected from the FM side, with spin $\sigma=\uparrow,\downarrow$, the excitation energy E, and the wave vector $\boldsymbol{k}_\sigma^e$, at an angle θ from the interface normal, there are four reflection processes: (i) Andreev reflection to the majority spin ($r_h^\uparrow$), (ii) Andreev reflection to the minority spin ($r_h^\downarrow$), (iii) normal reflection to the majority spin ($r_e^\uparrow$), and (iv) normal reflection to the minority spin ($r_e^\downarrow$) (see Fig. 1). The Andreev and normal-reflection coefficients are denoted by r_h^σ and r_e^σ, respectively. Solving the BdG equation, the wave function is $\Psi(\boldsymbol{r})=\Psi(x)e^{i\boldsymbol{k}_\parallel \boldsymbol{r}_\parallel}$, where $\boldsymbol{r}_\parallel$ is parallel to the interface, and

$$\begin{aligned}\Psi_{\mathrm{FM}}(x) = {} & \begin{pmatrix} s \\ 0 \\ 0 \\ 0 \end{pmatrix} e^{ik_\uparrow^e \cos\theta x} + \begin{pmatrix} 0 \\ \bar{s} \\ 0 \\ 0 \end{pmatrix} e^{ik_\downarrow^e \cos\theta x} + r_e^\uparrow \begin{pmatrix} 1 \\ 0 \\ 0 \\ 0 \end{pmatrix} e^{-ik_\uparrow^e A x} \\ & + r_e^\downarrow \begin{pmatrix} 0 \\ 1 \\ 0 \\ 0 \end{pmatrix} e^{-ik_\downarrow^e \bar{A} x} + r_h^\uparrow \begin{pmatrix} 0 \\ 0 \\ 1 \\ 0 \end{pmatrix} e^{ik_\uparrow^h \cos\theta_\uparrow^h x} \\ & + r_h^\downarrow \begin{pmatrix} 0 \\ 0 \\ 0 \\ 1 \end{pmatrix} e^{ik_\downarrow^h \cos\theta_\downarrow^h x} \end{aligned} \tag{3}$$

on the FM side. The notations are as follows: the quasiparticle wave vectors are given by

$$k_\uparrow^{e(h)} = \sqrt{2m[E_{\mathrm{FM}} + (-)E + h_0]},$$

$$k_\downarrow^{e(h)} = \sqrt{2m[E_{\mathrm{FM}} + (-)E - h_0]}.$$

An incoming electron with spin $\uparrow$ is described by $s=1,\bar{s}=0$, while a spin $\downarrow$ electron is described by $s=0,\bar{s}=1$. Then, $A = s\cos\theta + \bar{s}\cos\theta_\uparrow^e$ and $\bar{A}=\bar{s}\cos\theta + s\cos\theta_\downarrow^e$ and $\theta_\sigma^{e(h)}$ are angles between the wave vectors $\boldsymbol{k}_\sigma^{e(h)}$ and the interface normal.

Similarly, the BdG wave function on the superconducting side is given by

$$\Psi_{SC}(x) = \frac{t_e^{\uparrow}}{\sqrt{2}}\begin{pmatrix} u \\ -ie^{i\theta_1^e}u \\ ie^{i\theta_1^e}v \\ v \end{pmatrix} e^{ik_1^e \cos\theta_1^e x} + \frac{t_e^{\downarrow}}{\sqrt{2}}\begin{pmatrix} u \\ ie^{i\theta_2^e}u \\ -ie^{i\theta_2^e}v \\ v \end{pmatrix} e^{ik_2^e \cos\theta_2^e x} + \frac{t_h^{\uparrow}}{\sqrt{2}}\begin{pmatrix} v \\ ie^{-i\theta_1^h}v \\ -ie^{-i\theta_1^h}u \\ u \end{pmatrix} e^{-ik_1^h \cos\theta_1^h x} + \frac{t_h^{\downarrow}}{\sqrt{2}}\begin{pmatrix} v \\ -ie^{-i\theta_2^h}v \\ ie^{-i\theta_2^h}u \\ u \end{pmatrix} e^{-ik_2^h \cos\theta_2^h x}, \quad (4)$$

with the wave vectors

$$k_1^{e(h)} = -m\gamma_0 + \sqrt{(m\gamma_0)^2 + 2m[E_{FS} + (-)\Omega]},$$

$$k_2^{e(h)} = m\gamma_0 + \sqrt{(m\gamma_0)^2 + 2m[E_{FS} + (-)\Omega]}$$

and $\Omega=\sqrt{E^2-\Delta_0^2}$. The transmission amplitudes of electronlike and holelike quasiparticles are t_e^{σ} and t_h^{σ}, respectively. The quasiparticle amplitudes in the NCSC region are given as

$$u = \frac{1}{\sqrt{2}}\sqrt{1+\frac{\Omega}{E}}, \quad v = \frac{1}{\sqrt{2}}\sqrt{1-\frac{\Omega}{E}}. \quad (5)$$

Finally, $\theta_{1(2)}^{e(h)}$ are the angles between the wave vectors $k_{1(2)}^{e(h)}$ and the interface normal, as shown in Fig. 1. The angles are obtained from the following equations:

$$(sk_{\uparrow}^e + \bar{s}k_{\downarrow}^e)\sin\theta = sk_{\downarrow}^e \sin\theta_{\downarrow}^e + \bar{s}k_{\uparrow}^e \sin\theta_{\uparrow}^e = k_{\sigma}^h \sin\theta_{\sigma}^h = k_{1(2)}^{e(h)} \sin\theta_{1(2)}^{e(h)}, \quad (6)$$

which express the conservation of the parallel component of the wave vector due to the translational symmetry along the interface.

All the coefficients in Eqs. (3) and (4) can be determined by the following boundary conditions for the wave functions:

$$\Psi_{FM}|_{x=0^-} = \Psi_{SC}|_{x=0^+}, \quad (7)$$

$$\hat{v}_x\Psi_{SC}|_{x=0^+} - \hat{v}_x\Psi_{FM}|_{x=0^-} = -2iU_0\eta\Psi_{FM}|_{x=0^-}, \quad (8)$$

where η is the 4×4 matrix

$$\eta = \begin{pmatrix} 1 & 0 & 0 & 0 \\ 0 & 1 & 0 & 0 \\ 0 & 0 & -1 & 0 \\ 0 & 0 & 0 & -1 \end{pmatrix} \quad (9)$$

and the velocity operator in the x direction is defined as[31]

$$\hat{v}_x = \begin{pmatrix} -\frac{i}{m}\frac{\partial}{\partial x} & i\gamma_0\theta(x) & 0 & 0 \\ -i\gamma_0\theta(x) & -\frac{i}{m}\frac{\partial}{\partial x} & 0 & 0 \\ 0 & 0 & \frac{i}{m}\frac{\partial}{\partial x} & -i\gamma_0\theta(x) \\ 0 & 0 & i\gamma_0\theta(x) & \frac{i}{m}\frac{\partial}{\partial x} \end{pmatrix}. \quad (10)$$

Note that the presence of the spin-orbit coupling results in the off-diagonal components of the velocity operator. We also introduce the dimensionless parameters $Z=2mU_0/k_{FS}$ and $\alpha=2m\gamma_0/k_{FS}$, characterizing the barrier strength and the magnitude of the RSOC, respectively.

By using the general BTK formalism,[28] we obtain for the dimensionless differential tunneling conductance,

$$G(E) = \sum_{\sigma} P_{\sigma}G_{\sigma}(E),$$

$$G_{\sigma}(E) = \frac{1}{G_N}\int_{\theta_c} d\theta \cos\theta G_{\sigma}(E,\theta),$$

$$G_N = \int_{\theta_c} d\theta \cos\theta \frac{4\cos^2\theta}{4\cos^2\theta + Z^2}, \quad (11)$$

where $P_{\sigma}=\frac{1}{2}(1+\sigma h_0/E_{FM})$ is the probability that an incident electron has spin σ [$P_{\uparrow}\neq P_{\downarrow}$ because of the difference between the densities of states in the spin-$\uparrow$ and spin-$\downarrow$ bands (see Ref. 7)], G_N is the tunneling conductance for a normal-metal/normal-metal junction, and θ_c is determined by the angle of total reflection (critical angle) for incident electron with spin σ. For an incoming electron with spin $\uparrow$, the critical angles for the Andreev reflection and the transmission are given by $\theta_{c1}=\arcsin(k_{\downarrow}^h/k_{\uparrow}^e)$ and $\theta_{c2}=\arcsin(k_1^{e(h)}/k_{\uparrow}^e)$, respectively. When θ exceeds θ_{c1}, the x component of the wave vector in the AR process, $\sqrt{(k_{\downarrow}^h)^2-(k_{\uparrow}^e)^2\sin^2\theta}$, becomes purely imaginary so that the Andreev-reflected quasiparticles do not contribute to the charge current. Further, when $\theta > \theta_{c2}$, the transmitted quasiparticles with the wave vectors $k_1^{e(h)}$ do not contribute to the conductance.

The conductance for an electron with spin σ as a function of the excitation energy E and the incident angle θ reads

$$G_{\sigma}(E,\theta) = 1 + \frac{\lambda_1}{\lambda_0}|r_h^{\uparrow}|^2 + \frac{\lambda_2}{\lambda_0}|r_h^{\downarrow}|^2 - \frac{\lambda_3}{\lambda_0}|r_e^{\uparrow}|^2 - \frac{\lambda_4}{\lambda_0}|r_e^{\downarrow}|^2. \quad (12)$$

The ratios of λ_i on the right-hand side of this equation are obtained from the conservation of probability,

$$\lambda_0 = (sk_{\uparrow}^e + \bar{s}k_{\downarrow}^e)\cos\theta, \quad \lambda_1 = k_{\uparrow}^h \cos\theta_{\uparrow}^h,$$

$$\lambda_2 = k_{\downarrow}^h \cos\theta_{\downarrow}^h, \quad \lambda_3 = k_{\uparrow}^e A, \quad \lambda_4 = k_{\downarrow}^e \bar{A}.$$

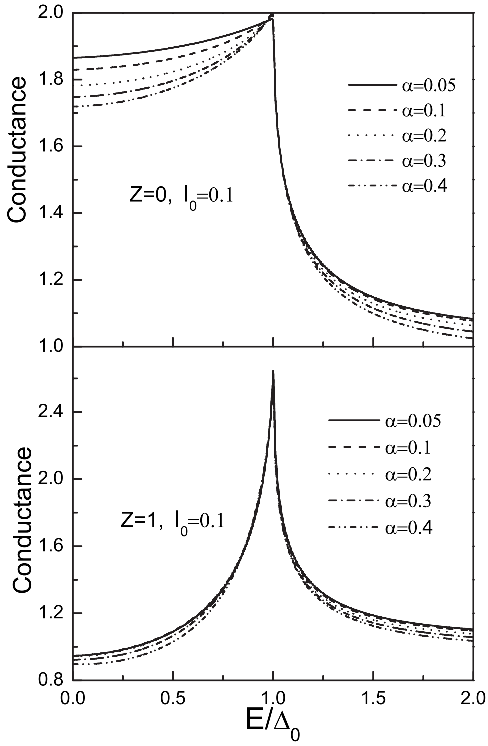

FIG. 2. The conductance $G(E)$ versus the dimensionless energy E/Δ_0 for $I_0=0.1$, $R=1$, and different values of the RSOC: $\alpha=0.05$, 0.1, 0.2, 0.3, and 0.4. $Z=0$ (top panel) and $Z=1$ (bottom panel).

III. RESULTS AND DISCUSSION

In this section, we present the results of numerical calculations for the conductance of the FM/NCSC junction at zero temperature, plotted as a function of the dimensionless quasiparticle energy E/Δ_0. We will study the effects on the tunneling conductance of three dimensionless parameters: the Rashba spin-orbit coupling α, the exchange energy $I_0 = h_0/E_{\mathrm{FM}}$, and the Fermi wave-vector mismatch R. In our calculation, we choose $\Delta_0/E_{FS}=0.01$ and consider two cases: $Z=0$, which corresponds to a negligible potential barrier at the interface, and also $Z=1$, corresponding to a high-transparency interface, which is often realized in the scanning tunneling microscopy experiments.

We consider first the case in which there is no Fermi-surface mismatch, i.e., $E_{\mathrm{FM}}=E_{FS}$ and $R=1$. Figure 2 displays the behavior of the tunneling conductance $G(E)$ at a fixed small exchange-energy value of $I_0=0.1$ for several values of α. In the absence of the interface barrier ($Z=0$), the results are shown in the top panel. One can see clearly that the curves there are similar to the well-known BTK results.[28] In the BTK model, the conductance in the subgap region, $0 \leq E \leq \Delta_0$, for the materials with $I_0=\alpha=0$ is equal to 2 due to the Andreev reflection. One can see that our curves in the top panel indeed approach this value (and are all close to 2 at the gap edge, i.e., at $E=\Delta_0$). That the subgap conductance is slightly smaller than 2 can be attributed to the suppression of the Andreev reflection due to the different densities of states in the spin-up and spin-down bands. The conductance at zero energy and also far away from the gap edge monotonically decreases with increasing the RSOC in the NCSC. This can be understood as follows: as α increases, the transmitted waves with the wave vectors $k_1^{e(h)}$ quickly become evanescent since the angle of total reflection θ_{c2} for the waves with $k_1^{e(h)}$ decreases as α increases. The eigenstates corresponding to such waves can no longer contribute to the conductance. In the bottom panel of Fig. 2, $Z=1$, the conductance curves display similar behavior but with a stronger suppression of $G(E)$ in the subgap region and a higher and sharper maximum at the gap edge $E=\Delta_0$.

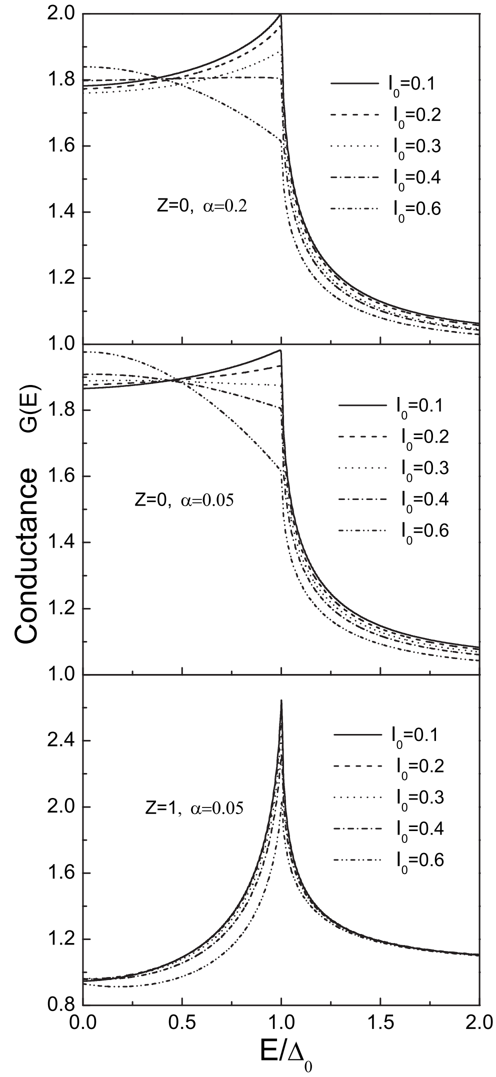

FIG. 3. The conductance $G(E)$ versus the dimensionless energy E/Δ_0 for $R=1$ and different values of the exchange energy: $I_0 =0.1$, 0.2, 0.3, 0.4, and 0.6. $\alpha=0.2$, $Z=0$ (top panel), $\alpha=0.05$, $Z=0$ (middle panel), and $\alpha=0.05$, $Z=1$ (bottom panel).

We next consider the effect of the exchange energy on the tunneling conductance in the same situation as in Fig. 2, i.e., for $R=1$. In Fig. 3, the variation in $G(E)$ with E/Δ_0 is plotted for several values of I_0. In a FM/CSC junction, the conductance monotonically decreases with increasing I_0 (Refs. 7 and 8) because of the reduction in the Andreev reflection when only a small fraction of injected electrons from the majority-spin band can be reflected as holes belonging to the minority-spin band. However, if the superconductor has no inversion symmetry, the Fermi surface is split into two due to

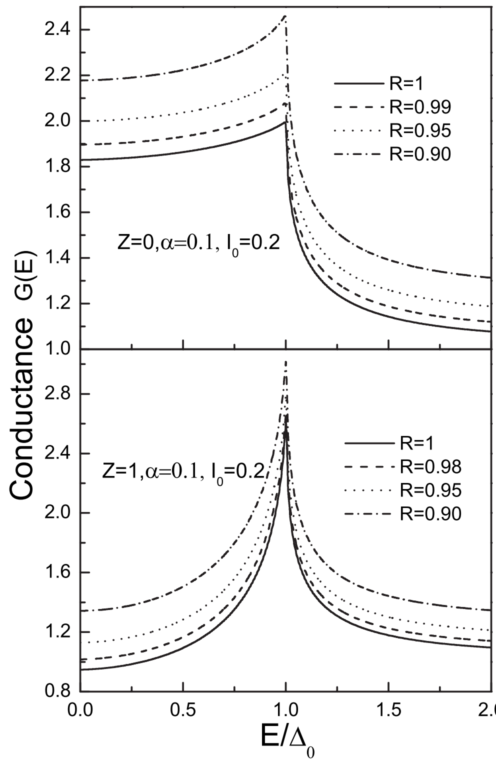

FIG. 4. The conductance $G(E)$ versus the dimensionless energy E/Δ_0 for $\alpha=0.1$, $I_0=0.2$, and different values of the Fermi wave-vector mismatch parameter: $R=1$, 0.98, 0.95, and 0.90. $Z=0$ (top panel) and $Z=1$ (bottom panel).

the spin-orbit coupling, thus making the conductance features more interesting. As seen clearly from the top ($\alpha=0.2$) and middle ($\alpha=0.05$) panels in Fig. 3, in the presence of the RSOC, the exchange energy can enhance the Andreev reflection and therefore the subgap conductance in the region $0\le E\le E^*$, where $E^*\simeq\Delta_0/2$. This effect becomes more pronounced at $\alpha=0.05$, in which case the subgap conductance at $E=0$ is monotonically enhanced for all values of I_0. The conductance can even have a maximum at $E=0$ at certain values of I_0 and α. These features are quite different from those observed in the FM/CSC junction where the peak stems from the interplay of the FWM and the exchange field.[11,12,29] When the interfacial scattering is nonzero, as shown in the bottom panel of Fig. 3, a rather sharp conductance peak appears at the gap edge. It becomes increasingly narrow as I_0 grows due to the suppression of the Andreev reflection. Furthermore, the exchange-energy dependence becomes weak in the region $E>\Delta_0$ and the conductance approaches its normal-state value $G(E)=1$ (Ref. 28) at higher excitation energies.

We now turn to the effects of the Fermi wave-vector mismatch, namely, $R\neq 1$, on the tunneling conductance. The difference in the Fermi energies in the FM and NCSC regions results in some interesting features in the conductance spectrum. In Fig. 4, which shows the results at $\alpha=0.1$, $I_0=0.2$, $Z=0$ (top panel), and $Z=1$ (bottom panel), we consider the evolution of the conductance curves for several values of the FWM. One can easily see that the conductance is monotonically enhanced in the whole region of excitation energies as the FWM parameter R decreases (i.e., the difference between $E_{\rm FM}$ and E_{FS} increases), which is significantly different from the case of a FM/CSC junction.[11,12,29] This result can be explained by the fact that in the presence of the RSOC, a smaller R will lead to the weaker ordinary scattering at the interface, which increases the Andreev reflection. We would like to point out that in the absence of the RSOC, one cannot obtain the monotonic increase in the conductance at all excitation energies by varying R and/or I_0. At energies much higher than the gap edge, $G(E)$ approaches 1, i.e., its normal-state value.

IV. SUMMARY

To summarize our results, we have investigated the tunneling conductance of the FM/NCSC junction with the help of the extended BTK formalism. Our results show a number of features in $G(E)$ that are qualitatively different from the previously studied cases of N/NCSC and FM/CSC junctions. These are caused by the interplay between the Rashba spin-orbit coupling in the noncentrosymmetric superconductor, the exchange energy in the ferromagnet, and the Fermi wave-vector mismatch between the two regions.

If the Fermi energies in FM and NCSC regions are the same, then far from the gap edge the conductance is monotonically enhanced by introducing a small RSOC, while around the gap edge the conductance is almost independent of RSOC. In addition, the subgap conductance can be enhanced due to the interplay of the RSOC and the exchange energy and can have a maximum at $E=0$ at certain values of α and I_0. The enhancement of the conductance is more pronounced at smaller α, which is attributed to the increase in the Andreev reflection by the small RSOC dominating the decrease due to the exchange energy. These phenomena are essentially different from those found in FM/CSC junctions, where both the enhanced subgap conductance and its maximum arise from the effect of the FWM at a fixed exchange energy.

We also considered the case of different Fermi energies in the FM and NCSC regions. The tunneling conductance is quite sensitive to the FWM and displays a monotonic increase as the difference between the Fermi energies increases due to the suppressed ordinary scattering at the interface and enhanced Andreev reflection. This behavior is also essentially different from that in FM/CSC junctions.

As for the experimental situation, while we are not aware of any work done on FM/NCSC junctions, FM/CSC junctions have been studied in Refs. 4–6. In those works, the spin polarization of the current in the ferromagnet (the transport spin polarization) was determined by analyzing the experimental data within the extended BTK scheme, with the total current decomposed into unpolarized and fully polarized components. Our model, which includes the RSOC, can also be used in the context of spin-polarized tunneling spectroscopy.

ACKNOWLEDGMENTS

This work was supported by a Discovery Grant from the Natural Sciences and Engineering Research Council of Canada.

[1] C. R. Hu, Phys. Rev. Lett. **72**, 1526 (1994).
[2] S. Kashiwaya, Y. Tanaka, M. Koyanagi, and K. Kajimura, Phys. Rev. B **53**, 2667 (1996).
[3] J. W. Ekin, Y. Xu, S. Mao, T. Venkatesan, D. W. Face, M. Eddy, and S. A. Wolf, Phys. Rev. B **56**, 13746 (1997).
[4] S. K. Upadhyay, A. Palanisami, R. N. Louie, and R. A. Buhrman, Phys. Rev. Lett. **81**, 3247 (1998).
[5] R. J. Soulen, Jr., J. M. Byers, M. S. Osofsky, B. Nadgorny, T. Ambrose, S. F. Cheng, P. R. Broussard, C. T. Tanaka, J. Nowak, J. S. Moodera, A. Barry, and J. M. D. Coey, Science **282**, 85 (1998).
[6] P. Raychaudhuri, A. P. Mackenzie, J. W. Reiner, and M. R. Beasley, Phys. Rev. B **67**, 020411(R) (2003).
[7] M. J. M. de Jong and C. W. J. Beenakker, Phys. Rev. Lett. **74**, 1657 (1995).
[8] J.-X. Zhu, B. Friedman, and C. S. Ting, Phys. Rev. B **59**, 9558 (1999).
[9] T. Hirai, Y. Tanaka, N. Yoshida, Y. Asano, J. Inoue, and S. Kashiwaya, Phys. Rev. B **67**, 174501 (2003).
[10] J. Linder and A. Sudbø, Phys. Rev. B **75**, 134509 (2007).
[11] I. Žutić and O. T. Valls, Phys. Rev. B **60**, 6320 (1999).
[12] I. Žutić and O. T. Valls, Phys. Rev. B **61**, 1555 (2000).
[13] G. Sun, D. Y. Xing, J. M. Dong, and M. Liu, Phys. Rev. B **65**, 174508 (2002).
[14] Y. C. Tao and J. G. Hu, J. Appl. Phys. **104**, 063903 (2008).
[15] Z.-Y. Zhang, Eur. Phys. J. B **63**, 65 (2008).
[16] E. Bauer, G. Hilscher, H. Michor, Ch. Paul, E. W. Scheidt, A. Gribanov, Yu. Seropegin, H. Noël, M. Sigrist, and P. Rogl, Phys. Rev. Lett. **92**, 027003 (2004).
[17] L. P. Gor'kov and E. I. Rashba, Phys. Rev. Lett. **87**, 037004 (2001).
[18] S. K. Yip, Phys. Rev. B **65**, 144508 (2002).
[19] K. V. Samokhin, Phys. Rev. Lett. **94**, 027004 (2005); Phys. Rev. B **76**, 094516 (2007).
[20] V. M. Edelstein, Phys. Rev. Lett. **75**, 2004 (1995).
[21] S. Fujimoto, Phys. Rev. B **72**, 024515 (2005).
[22] D. F. Agterberg, Physica C **387**, 13 (2003).
[23] K. V. Samokhin, Phys. Rev. B **70**, 104521 (2004).
[24] R. P. Kaur, D. F. Agterberg, and M. Sigrist, Phys. Rev. Lett. **94**, 137002 (2005).
[25] T. Yokoyama, Y. Tanaka, and J. Inoue, Phys. Rev. B **72**, 220504(R) (2005).
[26] C. Iniotakis, N. Hayashi, Y. Sawa, T. Yokoyama, U. May, Y. Tanaka, and M. Sigrist, Phys. Rev. B **76**, 012501 (2007).
[27] J. Linder and A. Sudbø, Phys. Rev. B **76**, 054511 (2007).
[28] G. E. Blonder, M. Tinkham, and T. M. Klapwijk, Phys. Rev. B **25**, 4515 (1982).
[29] P. H. Barsic and O. T. Valls, Phys. Rev. B **79**, 014502 (2009).
[30] T. Yokoyama, Y. Tanaka, and J. Inoue, Phys. Rev. B **74**, 035318 (2006).
[31] L. W. Molenkamp, G. Schmidt, and G. E. W. Bauer, Phys. Rev. B **64**, 121202(R) (2001).